Unit Commitment With Continuous-Time Generation and Ramping Trajectory Models

Masood Parvania, *Member, IEEE*, and Anna Scaglione, *Fellow, IEEE*

***Abstract*—There is increasing evidence of shortage of ramping resources in the real-time operation of power systems. To explain and remedy this problem systematically, in this paper we take a novel look at the way the day-ahead unit commitment (UC) problem represents the information about load, generation and ramping constraints. We specifically investigate the approximation error made in mapping of the original problem, that would decide the continuous-time generation and ramping trajectories of the committed generating units, onto the discrete-time problem that is solved in practice. We first show that current practice amounts to approximating the trajectories with linear splines. We then offer a different representation through cubic splines that provides physically feasible schedules and increases the accuracy of the continuous-time generation and ramping trajectories by capturing sub-hourly variations and ramping of load in the day-ahead power system operation. The corresponding day-ahead UC model is formulated as an instance of mixed-integer linear programming (MILP), with the same number of binary variables as the traditional UC formulation. Numerical simulation over real load data from the California ISO demonstrate that the proposed UC model reduces the total day-ahead and real-time operation cost, and the number of events of ramping scarcity in the real-time operations.**

***Index Terms*—Continuous-time function space, generation trajectory, mixed-integer linear programming, ramping trajectory, unit commitment.**

I. Introduction

POWER system operation planning is a continuous-time, stochastic, mixed integer optimization problem that is broken into different time scales, each mapped into a corresponding discrete time approximation, taking care of certain finite set of commitment variables and operation schedules. The time horizons go from several days ahead to the real-time operation of few seconds ahead. In a market-based framework for trading electricity, the generation scheduling problem is processed in multiple forward and real-time markets. Among the markets, it is in the day-ahead market that most of the electricity trading occurs.

The day-ahead market clearing is handled by solving the unit commitment (UC) problem which schedules the most economic set of generating units on an hourly basis, to meet the hourly forecasted load for the next day [1]. Because of its pivotal role, the study of the UC problem formulation and solution has been a very active area of research and development. An efficient formulation for the day-ahead UC problem, proposed in [2], [3], is an instance of mixed-integer linear programming (MILP) in which the generation cost function and operating constraints, and the transmission DC power flow constraints are linear with respect to all decision variables. The formulation was simplified in [4] reducing the number of integer variables. Another line of research is focused on modeling emerging energy resources in the UC problem, adding new cost terms and constraints and evaluating their impact on the system efficiency. For instance, [5] modeled flexible generating units (e.g., fuel switching and fuel-blending capabilities, combined cycle units), [6] modeled demand response assets used as contingency reserves to enhance system security, and many others.

The current hourly day-ahead UC of sampling hourly the demand and having two hourly decision variables per generating unit, i.e., the hourly commitment status and generation schedule, has worked well for compensating the variability and uncertainty of load. However, this practice is starting to fall short as increasing renewable energy resources add variability to the system and events of large shortfalls or surpluses occur much more frequently [7]–[10].

There have been notable research efforts for advancing the UC problem to cope with renewable integration problems. For example, in [11] a security-constrained UC algorithm was developed that takes into account the intermittency and volatility of wind power generation. A day-ahead UC model with stochastic security was formulated in [12] which is capable of accounting for non-dispatchable and variable wind power generation. Most recently, the research efforts have been focused on developing new operation models, market mechanisms and services to better take care of fast sub-hourly ramping of renewable resources. The Midcontinent ISO (MISO) and the California ISO (CAISO) are proposing new flexible ramping products to address this operational challenge. In the MISO, the flexible ramping product is designed to cover the net-load uncertainty in the next 10 minutes [13], [14]. In the CAISO, the flexible ramping product is designed to provide load following flexibility for the next 5 minutes and may look ahead several intervals [15], [16]. In [17], an optimization-based model is used to evaluate the ramping capability requirement considering both

Manuscript received April 10, 2015; revised July 08, 2015; accepted August 25, 2015. Date of publication October 26, 2015; date of current version May 02, 2016. This work was supported in part by the Department of Energy Consortium for Electric Reliability and Technology and in part by the National Science Foundation under Grant numbers 1549924 and 1549923. Patent Pending. Paper no. TPWRS-00481-2015.

M. Parvania is with the Department of Electrical and Computer Engineering, University of Utah, Salt Lake City, UT 84112 USA (e-mail: masood.parvania@utah.edu).

A. Scaglione is with the School of Electrical, Computer and Energy Engineering, Arizona State University, Tempe, AZ 85287 USA (e-mail: anna.scaglione@asu.edu).

Color versions of one or more of the figures in this paper are available online at http://ieeexplore.ieee.org.

Digital Object Identifier 10.1109/TPWRS.2015.2479644

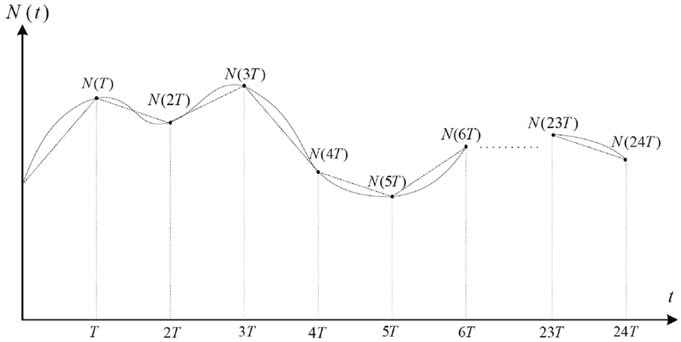

Fig. 1. Linear spline approximation of the continuous load profile.

security and economics. In [18], a deterministic ramping capability model with transmission constraint is proposed to ensure its deliverability. In [19], both the deterministic and stochastic models are evaluated in designing the market for flexible ramping products. In [20], a robust economic dispatch model is developed with ramping capability requirement and compared with the deterministic model. However, defining new ramping services, like a flexible ramping product, complicates the market structure, and raises questions about what is the reasonable level of cost allocation on these new market products.

The actual real-time load of power system can be divided to a part that is scheduled for in day-ahead operation, and the deviation between the day-ahead load profile and the real-time load that needs to be supplied by the available resources at the subsequent stages of operation, depending to different ISOs' market structure. The real-time load deviation results from two kinds of error in day-ahead load profile: 1) error due to the imperfect forecast, 2) error due to the day-ahead load profile approximation. Here, we argue that the ramping scarcity problems are originated, partly, due to the inherent error in current practice of day-ahead load profile approximation. In fact, ramping events and constraints are inter-temporal continuous-time mathematical objects. The natural implication of the current UC formulation is that, within the hour, generators shall follow a linear ramp from one value to the next. Intuitively, looking at Fig. 1, the linear trajectory does not fully capture the prior information about sub-hourly variations of the net-load and one must expect deviation which will have to be handled in the real-time operation. If this short-term deviation is beyond the coverage of the hourly day-ahead dispatch decisions, the short-term operations may be left with sufficient capacity but without ramping capability to respond to sub-hourly net-load variations, as was observed by multiple ISOs [14], [15], with obviously undesirable economic and security consequences.

These observations demonstrate that the current hourly day-ahead UC model does not efficiently utilize the available ramping capability of the generation resources and the prior information about the load. The question, that this work tries to address, is twofold: 1) whether or not the problems we are experiencing (e.g., ramping scarcity events) are tied to the inherent errors in our discrete-time approximation of ramps, and 2) if forecasts of hourly samples incorporate all the information about the variability expected in the net-load.

A. Contribution and Paper Structure

To address the questions posed above we propose and analyze a different approach to sampling the information and decision variables in the day-ahead UC problem. The main goal of our proposed UC model is to reduce the approximation error in describing the continuous-time ramping phenomena in the day-ahead operation, capturing more accurately the essential information available about the day-ahead net-load evolution in time, while revealing the potential operational flexibility of generating units that have significant impact on the day-ahead operation solution, but is not captured by current UC formulation. In this paper, the continuous-time variations of generation trajectory are modeled by representing the decision variables for generating units as the coefficients of a cubic Hermite splines expansion. The cubic Hermite spline coefficients represent the generation value and its derivative (i.e., ramp) at the starting and ending point of the scheduling intervals. We also define and model the continuous-time ramping trajectory of generating units as the derivative of the generation trajectory. In order to incorporate the continuous-time generation and ramping trajectory models in the UC problem, a function space-based optimization model is proposed that models all the prevailing UC constraints and the generation cost function using the coefficients of generation trajectory model in the function space of cubic Hermite spline. The application of our proposed UC model would modify the day-ahead commitment and schedule of generating units, and would line up the generation fleet in such a way that the composition of online units is better prepared to respond to the sub-hourly variations of the net-load in real-time operation.

The rest of the paper is organized as follows: Section III presents the interpretation of the current UC model in the function space of linear splines. The proposed models for continuous-time generation and ramping trajectories of generating units are presented in Section IV. Section V presents the proposed UC model that integrates the continuous-time generation and ramping trajectories. The numerical simulations using the real load data of CAISO is presented in Section VI, and finally the conclusions and future works are discussed in Section VII.

B. Notation

The following notation is utilized throughout the paper: boldface letters indicate vectors and matrices, while the lower case letters indicate scalar values. The subscripts k, m, n respectively are the indexes of generating units, time intervals (hours), and the segments in the linearize cost function. The letters N, G, I, Γ, γ, respectively indicate the net-load, generation, commitment variables, auxiliary generation variables, and linearized cost function derivatives in each range (i.e., prices), while to refer to the whole cost functions we use the letter C. Capacity limits are marked with the superscripts max and min. We use $B_q(t)$, $H_{i,j}(t)$ with $i, j \in \{0, 1\}$, to refer to Bernstein polynomials and cubic Hermite polynomials, and place superscripts B and H to distinguish the load and generation coefficients of their trajectory expressed as a linear combination on such polynomials. Continuous time is t, a specific time is t_m (i.e., the hour) and the letter τ_m is used to refer to a specific function of time that is the argument of the polynomial basis used for the representation of load and/or generation trajectory within a certain

mth interval, while $T_m = t_m - t_{m-1}$. Startup and shutdown are marked by SU, SD respectively, used as superscripts for costs and ramping constraints, where the letter R is used. Minimum On/Off Time are T_{on} and T_{off}.

II. Generation Trajectory From the Current UC

The notion of generation trajectory has not been given detailed attention in day-ahead power system operation, and there is not uniform agreement on the definition/model of the day-ahead ramping trajectory of generating units. The current UC practice is to provide hourly constant schedules for the energy produced by the generating units during the hour. This could be interpreted as scheduling a piecewise constant trajectory, as ISOs and technical papers often indicate (see e.g., [2], [3], [21]). The area of the piecewise constant generation trajectory in an hour is the actual energy that is scheduled for each generating unit in the day-ahead operation. A strict interpretation of such piecewise constant generation trajectory (i.e., taking its time derivative) would imply that at the beginning of each hour generating units should instantly jump to the next hour schedule, which is not physically feasible nor it is compatible with how the schedule ramping constraints are enforced. In practice, subsequent real-time operation instructions are dispatched to make a smooth transition between the hourly constant schedules. For instance, CAISO instructs a 20-min linear ramp across hourly boundaries, where the generating units should start ramping 10 minutes before the next hour schedule until 10 minutes after [21]. However, this operation instruction is an ex-post instruction that is not co-optimized along with the day-ahead scheduling decisions, so it is not capable of affecting and improving the day-ahead UC decisions.

Alternately, the generation trajectory of units can be interpreted as being consistent with the hourly ramping constraint in the current UC formulation that is modeled as finite difference between two consecutive hourly generation schedules. This ramping constraint implies that the generating units follow a linear trajectory from a hourly generation schedule to the next, meaning that its derivative, i.e., the ramping trajectory, is a piecewise constant curve. In the next Section III, we mathematically formalize the linear interpretation of generation trajectory in current UC formulation. This helps explaining more easily our idea of using third order polynomials to discretize the decisions on the continuous-time generation trajectory, which is described in Section IV.

III. Continuous-Time Generation Trajectory

The day-ahead UC problem is a continuous-time optimization problem in nature, expressed as follows:

$$\begin{aligned} &\min \int_{\Omega} C(\mathbf{G}(t), \mathbf{I}(t)) dt \\ &\text{s.t.} f(\mathbf{G}(t), \mathbf{I}(t)) = 0 \\ &\qquad h(\mathbf{G}(t), \mathbf{G}'(t), \mathbf{I}(t)) \leq 0 \end{aligned} \tag{1}$$

where the objective is to minimize the total continuous-time generation cost of generating units over the day-ahead scheduling horizon Ω including the startup and shutdown costs; $\mathbf{G}(t)$, $\mathbf{G}'(t)$ and $\mathbf{I}(t)$ respectively represent the vector of continuous-time generation trajectory, continuous-time ramping trajectory, and the continuous-time binary commitment variables; $f(\cdot)$ and $h(\cdot)$ are respectively the prevailing UC equality and inequality constraints, including balance constraint, and generating units' capacity, ramping, minimum on/off time, and startup and shutdown cost constraints.

The conversion from continuous-time generation trajectory and commitment variables to discrete variables is based on the notion that the continuous-time variables lie in a Hilbert function space with countable dimensions [22]. In the current market practice, the variables $\mathbf{I}(t)$ are limited to hourly changes of commitment status. The continuous-time generation trajectory variable $\mathbf{G}(t)$, though, is flexible to change between two consecutive hourly schedules. Next we first show that the hourly day-ahead schedule of generating units and hourly day-ahead load forecast profiles of the current discrete-time UC solution (approximating (1)) lie in a linear function space. Since all polynomial splines of the same order are equivalent (they span the same sub-space), we choose to interpret the generation schedule, constraints and cost function in terms of shifts of Bernstein polynomials of degree 1.

A. Continuous-Time Model of Hourly Day-Ahead Load Profile

There are several different family of splines that can be used to approximate the continuous-time trajectory (space) of a data set with the desired level of accuracy, as the order of the basis grows [23], [24]. Among the polynomial splines, the Bernstein polynomials of degree n are defined as [23]:

$$B_{k,n}(t) = \binom{n}{k} t^k (1-t)^{n-k} \Pi(t), \quad k \in [0, n], t \in [0, 1). \tag{2}$$

When we are interested in the piecewise approximation of a set of data points, a bold feature of the Bernstein polynomials is that they can be utilized to more easily impose smoothness conditions not only at the break points but also inside the interval of interest, working only on the coefficients of the Bernstein spline expansion [23]. The linear spline approximation of the load shown in Fig. 1, can be mathematically expressed in each hourly sub-interval m in the function space of the two Bernstein polynomials of degree 1, i.e., $B_{0,1}(t) = t$ and $B_{1,1}(t) = 1 - t$, weighted by the value of load at the beginning and end of the hour, as follows:

$$\hat{N}(t) = N_m^{B0} B_{0,1}(t) + N_m^{B1} B_{1,1}(t), \quad t_m \leq t < t_{m+1} \tag{3}$$

where $N_m^{B0} = N(t_m)$ and $N_m^{B1} = N(t_{m+1})$ are the coefficients of the load representation in the linear function space. Defining the vectors:

$$\mathbf{B}_1(t) = (B_{0,1}(t); B_{1,1}(t))^T, \ \ \mathbf{N}_m = (N_m^{B0}, N_m^{B1})^T, \tag{4}$$

the linear expansion in (3) can be expressed in matrix form over the day-ahead scheduling horizon as

$$\hat{N}(t) = \sum_{m=0}^{M-1} \mathbf{B}_1^T(\tau_m) \mathbf{N}_m \tag{5}$$

where $\tau_m = (t - t_m)/(t_{m+1} - t_m)$ translates and rescales $\mathbf{B}_1(t)$ to cover each period $t_m \leq t \leq t_{m+1}$. The continuous-time load model in (5) represent the piecewise linear load profile in Fig. 1 in the $2M$-dimensional function space of the Bernstein polynomials of degree 1.

B. Continuous-Time Day-Ahead Generation Trajectory

The continuous-time generation trajectory corresponding to the discrete-time schedule of generating units is also an element of the same $2M$-dimensional function space spanned by $M = 24$ shifts of the Bernstein polynomials of degree 1, i.e.,

$$G_k(t) = \sum_{m=0}^{M-1} \mathbf{B}_1^T(\tau_m)\mathbf{G}_{k,m} \tag{6}$$

where $\mathbf{G}_{k,m} = (G_{k,m}^{B0}, G_{k,m}^{B1})^T$ represents the coefficients of the continuous-time generation trajectory of generating unit k at hourly interval m. In this case, the coefficients of the expansion equal to the hourly generation schedules:

$$G_{k,m}^{B0} = G_k(t_m),\ G_{k,m}^{B1} = G_k(t_{m+1}). \tag{7}$$

We note that although the continuous-time generation schedule lies in the $2M$-dimensional function space, the number of degrees of freedom is obviously M, due to generation continuity at the intersection of hourly intervals:

$$G_{k,m-1}^{B1} = G_{k,m}^{B0} = G_k(t_m), \quad \forall m > 1. \tag{8}$$

The quadratic cost function of generating units can be approximated by a piecewise linear cost function as follows to preserve the linearity of the UC formulation [4]:

$$C_k(G_k(t), I_k(t)) = C_k(G_k^{\min})I_k(t) + \sum_{n=0}^{N_k-1} \gamma_{k,n}(t)\Gamma_{k,n}(t) \tag{9}$$

where the capacity range of generating unit k is divided to N_k sections using intermediate generation points $g_0 = G_k^{\min}, g_1, g_2, \ldots, g_{N_k} = G_k^{\max}$, and N_k number of auxiliary generation variables $\Gamma_{k,n}(t)$ are defined to model the generation schedule in each of the linear sections. The total generation of generating unit k can be stated in terms of the auxiliary generation variables $\Gamma_{k,n}(t)$ as follows:

$$G_k(t) = G_k^{\min} I_k(t) + \sum_{n=0}^{N_k-1} \Gamma_{k,n}(t) \tag{10}$$

$$0 \le \Gamma_{k,n}(t) \le g_{n+1} - g_n. \tag{11}$$

The auxiliary generation variables $\Gamma_{k,n}(t)$ can be also expressed in the $2M$-dimensional function space spanned by $\{\mathbf{B}_1(\tau_m)\}_{m=0}^{M-1}$:

$$\Gamma_{k,n}(t) = \sum_{m=0}^{M-1} \mathbf{B}_1^T(\tau_m)\mathbf{\Gamma}_{k,n,m}. \tag{12}$$

The continuous-time relation in (10), is equivalent to the following constraint on the coefficients:

$$\mathbf{G}_{k,m} = G_k^{\min}\mathbf{I}_{k,m} + \sum_{n=0}^{N_k-1} \mathbf{\Gamma}_{k,n,m} \tag{13}$$

where $\mathbf{I}_{k,m} = (I_k(t_m), I_k(t_{m+1}))^T$, and $G_k^{\min}$ is the minimum generation capacity of unit k. We assume that the cost function coefficients $\gamma_{k,n}(t)$ in (9) are constant over each period, i.e.,

$$\gamma_{k,n}(t) \approx \gamma_{k,n}(t_m), \quad t_m \le t < t_{m+1}, \tag{14}$$

which is a fair assumption in an hourly market environment where the units offer bids for the hourly intervals. The total generation cost of generating unit k over the day-ahead scheduling horizon Ω can be calculated using the function space representation of $\Gamma_{k,n}(t)$ in (12) as follows:

$$\int_\Omega C_k(G_k(t), I_k(t))dt = \sum_{m=0}^{M-1} \left[C_k(G_k^{\min})I_k(t_m) + \sum_{n=0}^{N_k-1} \gamma_{k,n}(t_m)\Gamma_{k,n}(t_m) \right]. \tag{15}$$

In the following Section IV, we lift the order of the continuous-time representation of the load profile and for the corresponding generation trajectory using cubic splines.

IV. Cubic Spline Model of Generation Trajectory

In this section we propose to use the cubic spline function space for modeling continuous-time generation trajectory, in lieu of the linear splines. Cubic splines interpolates points with minimum curvature while providing additional flexibility to fit the continuous-time load variations [24]. Correspondingly, the load is also modeled through a cubic spline expansion.

We favor the expansion on two celebrated bases of cubic splines: the cubic Hermite basis and Bernstein polynomials of degree 3. The former are preferred because they allow us to define the coefficients of the expansion as samples of the generation and its rate of change, i.e., the ramp. The latter are useful as a proxy expansion to enforce the capacity and ramping constraints for the continuous-time generation trajectory, while working with the same number of coefficients.

Remark IV.1: Increasing the order of polynomials to approximate the load and model the continuous-time generation trajectory of units is a simple generalization of our idea, and may potentially capture more volatile load variations, reducing the approximation error in day-ahead load profile. However, as discussed in more detail in Section VI, this would increase the computation time of the resulting UC problem.

Let us start with the cubic Hermite splines model of the day-ahead load profile. Rather than sampling uniformly, we generalize the model and split the day-ahead scheduling horizon Ω into M intervals, using arbitrary points $0, t_1, t_2, \ldots, t_M$. The four cubic Hermite polynomial basis in $t \in [0, 1)$ are [24]:

$$\begin{aligned}
H_{00}(t) &= (2t^3 - 3t^2 + 1)\Pi(t)\\
H_{01}(t) &= (t^3 - 2t^2 + t)\Pi(t)\\
H_{10}(t) &= (-2t^3 + 3t^2)\Pi(t)\\
H_{11}(t) &= (t^3 - t^2)\Pi(t)
\end{aligned}$$

which are entries of the vector:

$$\mathbf{H}(t) = (H_{00}(t), H_{01}(t), H_{10}(t), H_{11}(t))^T.$$

The coefficients of the cubic Hermite approximation of load over the mth interval are denoted as the vector $\mathbf{N}_m^H = (N_m^{00}, N_m^{01}, N_m^{10}, N_m^{11})^T$, and the corresponding cubic Hermite approximation of the day-ahead load profile is:

$$\hat{N}(t) = \sum_{m=0}^{M-1} \mathbf{H}^T(\tau_m)\mathbf{N}_m^H. \tag{16}$$

The important feature of (16) is that the coefficients of the cubic Hermite approximation of load are uniquely defined by the value of load and the load derivative (i.e., ramp) at the starting and ending point of the intervals, i.e.,

$$N_m^{00} = \hat{N}(t_m),\ N_m^{10} = \hat{N}(t_{m+1}), \tag{17}$$

$$N_m^{01} = \hat{N}'(t_m),\ N_m^{11} = \hat{N}'(t_{m+1}). \tag{18}$$

The linear spline expansion only ensured continuity of the load but not of its derivative. The C^1 continuity [24] (i.e., continuity of the load and of the load derivative) in the cubic Hermite approximation is imposed through the constraint:

$$N_m^{00} = N_{m-1}^{10},\ \ N_m^{01} = N_{m-1}^{11} \quad \forall\, m > 0 \tag{19}$$

and implies that there are in reality $2M$ parameters defining $\hat{N}(t)$ in the function space of cubic Hermite splines.

Introducing $\mathbf{B_3}(t) = (B_{0,3}(t), B_{1,3}(t), B_{2,3}(t), B_{3,3}(t))^T$, the vector of Bernstein polynomials of degree 3, defined in (2) for $n = 3$, the cubic Hermite basis functions can be written in terms of Bernstein polynomials of degree 3 as follows [23]:

$$\mathbf{H}(t) = \mathbf{W}\mathbf{B_3}(t) \tag{20}$$

where the change of basis matrix $\mathbf{W}$ is:

$$\mathbf{W} = \begin{pmatrix} 1 & 1 & 0 & 0 \\ 0 & \frac{1}{3} & 0 & 0 \\ 0 & 0 & 1 & 1 \\ 0 & 0 & -\frac{1}{3} & 0 \end{pmatrix}. \tag{21}$$

Using (20), $\hat{N}(t)$ in (16) can be rewritten in terms of Bernstein polynomials of degree 3 as

$$\hat{N}(t) = \sum_{m=0}^{M-1} \mathbf{B}_3^T(\tau_m)\mathbf{W}^T\mathbf{N}_m^H = \sum_{m=0}^{M-1} \mathbf{B}_3^T(\tau_m)\mathbf{N}_m^B \tag{22}$$

where $\mathbf{N}_m^B = \mathbf{W}^T\mathbf{N}_m^H$ is the vector of coefficients for Bernstein polynomial approximation of the load in the mth interval.

Correspondingly, the continuous-time generation trajectory of units over the day-ahead scheduling horizon can be expressed as follows:

$$G_k(t) = \sum_{m=0}^{M-1} \mathbf{H}^T(\tau_m)\mathbf{G}_{k,m}^H = \sum_{m=0}^{M-1} \mathbf{B}_3^T(\tau_m)\mathbf{G}_{k,m}^B \tag{23}$$

where $\mathbf{G}_{k,m}^H = (G_{k,m}^{00}, G_{k,m}^{01}, G_{k,m}^{10}, G_{k,m}^{11})^T$ and $\mathbf{G}_{k,m}^B = (G_{k,m}^{B0}, G_{k,m}^{B1}, G_{k,m}^{B2}, G_{k,m}^{B3})^T$ are, respectively, the coefficients vectors of the cubic Hermite and Bernstein polynomial models of unit k in interval m, which are linearly related as $\mathbf{G}_{k,m}^B = \mathbf{W}^T\mathbf{G}_{k,m}^H$.

As shown in (23), the cubic Hermite spline and the Bernstein polynomial of degree 3 represent two interchangeable bases for modeling generation trajectory and we will switch between these two representations throughout the rest of the paper to enforce different constraints. To illustrate the relationship between the two sets of parameters, Fig. 2 shows the parameters of the two continuous-time generation trajectory models for an hypothetical generation trajectory. In Fig. 2(a), $G_{k,m}^{00}$ and $G_{k,m}^{10}$ are respectively the values of the generation at the beginning and ending points of the interval, while $G_{k,m}^{01}$ and $G_{k,m}^{11}$ represent the ramping of the generation trajectory at the beginning and ending points of the interval, respectively. The two Bernstein coefficients $G_{k,m}^{B0}$ and $G_{k,m}^{B3}$ in Fig. 2(b) are respectively equal to the cubic Hermite coefficients $G_{k,m}^{00}$ and $G_{k,m}^{10}$. The Bernstein point $G_{k,m}^{B1}$ is obtained by moving in the direction of the derivative in the beginning point for one third of the time interval, and the point $G_{k,m}^{B2}$ is obtained by moving in the opposite direction of the derivative in the ending point for one third of the time interval. This linear relationship between the two models is expressed in (23).

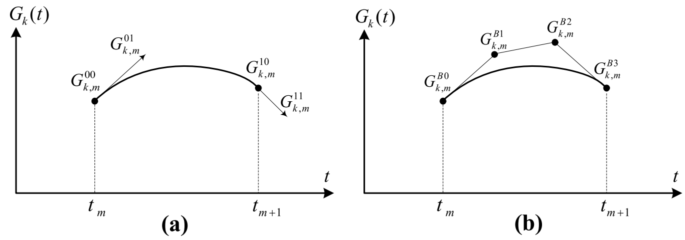

Fig. 2. Coefficients of a) cubic Hermite, b) Bernstein polynomials of degree 3.

The C^1 continuity property enforces that only the first two cubic Hermite coefficients, i.e., $G_{k,m}^{00}$ and $G_{k,m}^{01}$, are independent in each interval, which respectively represent the value of the generation and the generation ramping at the beginning point of the interval at time t_m. The two coefficients $G_{k,m}^{10}$ and $G_{k,m}^{11}$ in each interval are not independent and are respectively equal to the values of the generation and generation ramping at the beginning point of the subsequent interval.

The motivation for modeling the continuous-time generation trajectory of the generating units using the Bernstein polynomial of degree 3 in (23) is twofold. First, the derivatives of the Bernstein polynomials of degree n can be expressed as the degree of the polynomial, multiplied by the difference of two Bernstein polynomials of degree $n-1$ [23]. Specifically, for degree 3 we can write:

$$B'_{k,3}(t) = 3\big(B_{k-1,2}(t) - B_{k,2}(t)\big) \tag{24}$$

which can be written in matrix as follows:

$$\mathbf{B_3'}(t) = \mathbf{K}\mathbf{B_2}(t) \tag{25}$$

where $\mathbf{B_2}(t)$ is the vector of Bernstein polynomials of degree 2, and $\mathbf{K}$ is the linear matrix relating the derivatives of $\mathbf{B_3}(t)$ with $\mathbf{B_2}(t)$, defined as follows:

$$\mathbf{K} = \begin{pmatrix} -3 & 0 & 0 \\ 3 & -3 & 0 \\ 0 & 3 & -3 \\ 0 & 0 & 3 \end{pmatrix}. \tag{26}$$

Using (25), the *continuous-time ramping trajectory* of generating unit k can be defined in a space spanned by Bernstein polynomials of degree 2 as follows:

$$G'_k(t) = \sum_{m=0}^{M-1} \mathbf{B}_2^T(\tau_m)\mathbf{G'}_{k,m}^B \tag{27}$$

where $\mathbf{G}'^{B}_{k,m} = (G'^{B0}_{k,m}, G'^{B1}_{k,m}, G'^{B2}_{k,m})^T$ represents the vector of Bernstein coefficients of the continuous-time ramping trajectory, which can be expressed in terms of cubic Hermite splines as follows:

$$\mathbf{G}'^{B}_{k,m} = \mathbf{K}^T \mathbf{G}^{B}_{k,m} = \mathbf{K}^T \mathbf{W}^T \mathbf{G}^{H}_{k,m} \tag{28}$$

where

$$G'^{B0}_{k,m} = 3(G^{B1}_{k,m} - G^{B0}_{k,m}) = G^{01}_{k,m} \tag{29}$$

$$\begin{aligned} G'^{B1}_{k,m} &= 3(G^{B2}_{k,m} - G^{B1}_{k,m}) \\ &= 3(G^{10}_{k,m} - G^{00}_{k,m}) - G^{11}_{k,m} - G^{01}_{k,m} \end{aligned} \tag{30}$$

$$G'^{B2}_{k,m} = 3(G^{B3}_{k,m} - G^{B2}_{k,m}) = G^{11}_{k,m}. \tag{31}$$

The second motivation for using Bernstein polynomials is that the continuous-time generation and ramping trajectories satisfy the so called *convex hull property* [23], namely that the continuous-time trajectories will never be outside of the convex hull formed by the four Bernstein points, shown in Fig. 2(b). Accordingly, the lower and upper bounds of the continuous-time generation and ramping trajectories within the interval m can be respectively represented by the associated Bernstein coefficients in (32)–(35).

$$\min_{t_m \le t \le t_{m+1}} \{\mathbf{B}_3^T(\tau_m)\mathbf{G}^{B}_{k,m}\} \ge \min\{\mathbf{G}^{B}_{k,m}\} \tag{32}$$

$$\max_{t_m \le t \le t_{m+1}} \{\mathbf{B}_3^T(\tau_m)\mathbf{G}^{B}_{k,m}\} \le \max\{\mathbf{G}^{B}_{k,m}\} \tag{33}$$

$$\min_{t_m \le t \le t_{m+1}} \{\mathbf{B}_2^T(\tau_m)\mathbf{G}'^{B}_{k,m}\} \ge \min\{\mathbf{G}'^{B}_{k,m}\} \tag{34}$$

$$\max_{t_m \le t \le t_{m+1}} \{\mathbf{B}_2^T(\tau_m)\mathbf{G}'^{B}_{k,m}\} \le \max\{\mathbf{G}'^{B}_{k,m}\}. \tag{35}$$

One of the important advantages of the continuous-time modeling of generation trajectory using cubic Hermite and Bernstein polynomials in (23) is that the generation cost function (9) can be accurately computed for continuous-time generation trajectory, as opposed to the hourly constant generation schedule. At this regard, we also express the auxiliary generation variables $\Gamma_{k,n}(t)$ in the linearized cost function (9), in the function space of cubic Hermite polynomials as follows:

$$\Gamma_{k,n}(t) = \sum_{m=0}^{M-1} \mathbf{H}^T(\tau_m)\mathbf{\Gamma}^{H}_{k,n,m} \tag{36}$$

where $\mathbf{\Gamma}^{H}_{k,n,m}$ is the vector of their cubic Hermite coefficients:

$$\mathbf{\Gamma}^{H}_{k,n,m} = (\Gamma^{00}_{k,n,m}, \Gamma^{01}_{k,n,m}, \Gamma^{10}_{k,n,m}, \Gamma^{11}_{k,n,m})^T. \tag{37}$$

V. The Proposed Unit Commitment Model

In this section, we propose a function space-based UC formulation that incorporates the continuous-time generation and ramping trajectories developed in (23) and (27). The flow of data in the proposed model is shown in Fig. 3. The day-ahead load profile is approximated by the cubic Hermite polynomials as in (16), and the respective coefficients $\mathbf{N}^{H}_{m}$ are fed into the proposed UC model. The continuous-time generation and ramping trajectories of generating unit k are represented by the coefficients $\mathbf{G}^{H}_{k,m}$, $\mathbf{G}'^{B}_{k,m}$ defined over M intervals of the scheduling horizon Ω. The continuous-time binary commitment variable of generating unit k, $I_k(t)$, is assumed to be constant in each

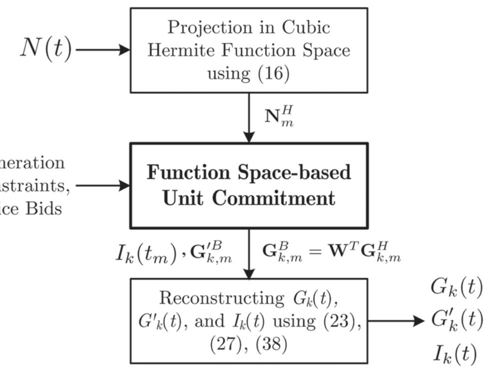

Fig. 3. The proposed UC model.

interval m, equaling to the commitment decision at the beginning of the interval $I_k(t_m)$, resulting in the following continuous-time piecewise constant representation of the commitment variable:

$$I_k(t) = \sum_{m=0}^{M-1} I_k(t_m)[u(t - t_m) - u(t - t_{m+1})]. \tag{38}$$

The coefficients $\mathbf{G}^{H}_{k,m}$, $\mathbf{G}'^{B}_{k,m}$ and the binary variables $I_k(t_m)$ act as the decision variables of the proposed UC model, and their optimal solution would be utilized to reconstruct the continuous-time generation and ramping trajectories of the generating units, as shown in Fig. 3. In the following, we formulate the elements of our proposed UC model.

A. Objective Function

As presented in (1), the objective of the UC problem is to minimize the total continuous-time generation cost of generating units over the scheduling horizon, including the startup and shutdown cost. The continuous-time generation cost function is derived in terms of the cubic Hermite coefficients of the auxiliary generation variables, $\mathbf{\Gamma}^{H}_{k,n,m}$, by integrating the linearized cost function in (9) as follows:

$$\begin{aligned} \int_{\Omega} \hat{C}_k(G_k(t), I_k(t))dt = \sum_{m=0}^{M-1} \Bigg[C_k(G_k^{\min}) \int_{t_m}^{t_{m+1}} I_k(t)dt \\ + \sum_{n=0}^{N_k-1} \gamma_{k,n}(t_m)(\mathbf{\Gamma}^{H}_{k,n,m})^T \left[\int_{t_m}^{t_{m+1}} \mathbf{H}(\tau_m)dt \right] \Bigg] \end{aligned} \tag{39}$$

where the cost coefficients $C_k(G_k^{\min})$ and $\gamma_{k,n}(t_m)$ are constant over each interval m. By calculating the integrals in (39), the objective function of the proposed UC model, including the total generation, startup and shutdown costs, can be written as follows:

$$\begin{aligned} \min \sum_{k=1}^{K} \sum_{m=0}^{M-1} \Bigg[C_k^{SU}(t_m) + C_k^{SD}(t_m) + T_m \Bigg(C_k(G_k^{\min}) I_k(t_m) \\ + \sum_{n=0}^{N_k-1} \gamma_{k,n}(t_m) \Bigg[\frac{\Gamma^{00}_{k,n,m} + \Gamma^{10}_{k,n,m}}{2} + \frac{\Gamma^{01}_{k,n,m} - \Gamma^{11}_{k,n,m}}{12} \Bigg] \Bigg) \Bigg]. \end{aligned} \tag{40}$$

The startup and shutdown costs in (40) are triggered when the units are committed or shutdown, which are respectively identified by the increment change in the binary variable in (41), (42).

In addition, the bounds of the auxiliary generation variables in (11) are translated in (43) into the constraints on the associated Bernstein coefficients, thanks to the convex hull property of the Bernstein polynomials explained in Section IV.

$$\gamma_k^{SU}\left[I_k(t_m)-I_k(t_{m-1})\right] \le C_k^{SU}(t_m) \quad \forall k, \forall m \tag{41}$$
$$\gamma_k^{SD}\left[I_k(t_{m-1})-I_k(t_m)\right] \le C_k^{SD}(t_m) \quad \forall k, \forall m \tag{42}$$
$$0 \le \mathbf{W}^T \mathbf{\Gamma}_{k,n,m}^H \le g_{n+1}-g_n \quad \forall n, \forall k, \forall m. \tag{43}$$

B. Balance and Generation Continuity Constraints

The continuous-time balance between generation and load is assured in (44) by balancing the four cubic Hermite coefficients of the continuous-time load and generation trajectory in each interval m. Unlike the current UC models where the generating units are scheduled to balance the hourly samples of load, the continuous-time generation trajectory would be scheduled in (44) to balance the continuous-time variations and ramping of load within the intervals, as represented by the cubic Hermite spline model. In addition, constraints (45) assure the C^1 continuity of the generation trajectory over the scheduling horizon. In (46), the Bernstein coefficient of the continuous-time generation trajectory of generating units, i.e., $\mathbf{W}^T \mathbf{G}_{k,m}^H$, are stated in terms of the coefficients of the auxiliary generation variables, where $\mathbf{I}_{k,m} = (I_k(t_m), I_k(t_m), I_k(t_{m+1}), I_k(t_{m+1}))^T$ is the vector of applicable binary variables. In (46), due to the C^1 continuity of the generation trajectory, the first two cubic Hermite coefficients of generation variables are associated with the commitment status of units in interval m, while the last two coefficients are associated with the commitment status of units in interval $m+1$.

$$\sum_{k=1}^{K} \mathbf{G}_{k,m}^H = \mathbf{N}_m^H \quad \forall m \tag{44}$$
$$G_{k,m}^{10} = G_{k,m+1}^{00}, G_{k,m}^{11} = G_{k,m+1}^{01} \quad \forall k, \forall m \tag{45}$$
$$\mathbf{W}^T \mathbf{G}_{k,m}^H = G_k^{\min} \mathbf{I}_{k,m} + \sum_{n=0}^{N_k-1} \mathbf{W}^T \mathbf{\Gamma}_{k,n,m}^H. \tag{46}$$

C. Generation Capacity and Ramping Constraints

As mentioned in Section IV, the convex hull property of Bernstein polynomials allow us to enforce the generation capacity constraint in continuous-time by capping the four Bernstein coefficients of the generation trajectory as follows:

$$\mathbf{W}^T \mathbf{G}_{k,m}^H \ge G_k^{\min} \mathbf{I}_{k,m} \quad \forall k, \forall m \tag{47}$$
$$\mathbf{W}^T \mathbf{G}_{k,m}^H \le G_k^{\max} \mathbf{I}_{k,m} \quad \forall k, \forall m. \tag{48}$$

The continuous-time ramping constraints can be applied in a similar way by capping the Bernstein coefficients of the continuous-time ramping trajectory of generating units derived in (29)–(31), only two of which are independent in each interval due to the ramping continuity constraint in (45). The ramping up and down constraints for the first Bernstein coefficient of generation ramping trajectory, (which also account for the startup and shutdown ramp rates) are defined as:

$$G_{k,m}^{\prime B0} \le R_k^U I_k(t_{m-1}) + R_k^{SU}[I_k(t_m) - I_k(t_{m-1})] + G_k^{\max}[1 - I_k(t_m)] \quad \forall k, \forall m \tag{49}$$

$$-G_{k,m}^{\prime B0} \le R_k^D I_k(t_m) + R_k^{SD}[I_k(t_{m-1}) - I_k(t_m)] + G_k^{\max}[1 - I_k(t_{m-1})] \quad \forall k, \forall m \tag{50}$$

where R_k^U, R_k^D, R_k^{SU}, R_k^{SD} respectively represent the ramp up, ramp down, startup ramp, and shutdown ramp limits of generating unit k. The ramping up and down constraints for the second Bernstein coefficient of generation ramping trajectory are defined as:

$$G_{k,m}^{\prime B1} \le R_k^U I_k(t_m) + \eta_1[1 - I_k(t_m)] \quad \forall k, \forall m \tag{51}$$
$$-G_{k,m}^{\prime B1} \le R_k^D I_k(t_{m+1}) + \eta_2[1 - I_k(t_{m+1})] \quad \forall k, \forall m = 0 \ldots M-2 \tag{52}$$

where η_1 and η_2 are constants and respectively equal to the upper bounds of $G_{k,m}^{\prime B1}$ and $-G_{k,m}^{\prime B1}$ in interval m when the unit is turning on and off in the subsequent interval. The second terms in the right-hand-side of (51) and (52) assure that the constraint does not prevent the unit from turning on and off, respectively.

D. Minimum On/Off Time Constraints

The minimum on and minimum off time constraints can be formulated as follows:

$$\sum_{m'=m}^{m+T_k^{\text{on}}-1} T_{m'} I_k(t_{m'}) \ge T_k^{\text{on}}[I_k(t_m) - I_k(t_{m-1})] \tag{53}$$
$$\sum_{m'=m}^{m+T_k^{\text{off}}-1} T_{m'}\left[1 - I_k(t_{m'})\right] \ge T_k^{\text{off}}\left[I_k(t_{m-1}) - I_k(t_m)\right] \tag{54}$$

where T_k^{on} and T_k^{off} represent the minimum on and off times of generating unit k.

In summary, (40)–(54) present our proposed UC model with continuous-time generation and ramping trajectory modeling which is formulated as a MILP problem and can be solved using any MILP solver. The solution of the proposed UC model would provide optimum continuous-time generation trajectory dispatch for each generating unit, in terms of the four cubic Hermite coefficients in each hour, as opposed to the hourly generation dispatch provided by the current UC model. The proposed UC model also provides the optimum continuous-time ramping trajectory for generating units that is unique to our approach.

VI. Numerical Results

To analyze and compare the UC formulations we use the data regarding 32 generating units of the IEEE Reliability Test System (RTS) [25] and load data from the CAISO. In Cases 1 and 2, we respectively study and analyze the results of running the current day-ahead (DA) UC model and our proposed UC with continuous-time generation and ramping trajectory models on the IEEE-RTS and CAISO load data. In both cases, we also simulated the real-time (RT) economic dispatch in five-minute intervals, which schedules for the deviations of day-ahead dispatch from the real-time five-minute load forecast data. Note that, depending on the market structure of different ISOs, there are additional scheduling stages between the day-ahead UC and RT economic dispatch, essentially trying to reduce the DA load deviations from the RT load. In addition, we assumed the real-time load deviation is served by the generating units

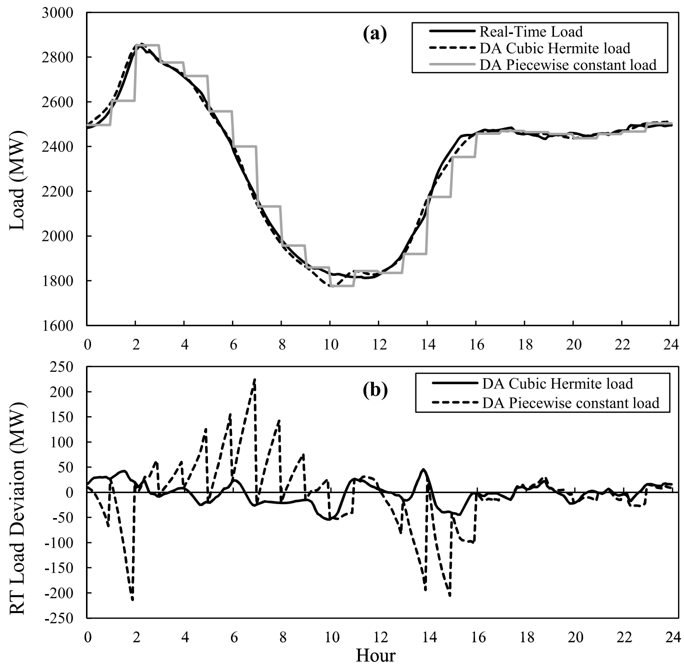

Fig. 4. (a) DA load profiles in Cases 1 and 2, (b) RT deviation from DA load profiles.

offering a single real-time energy bid equaling to 1.3 times their highest day-ahead energy offer. We took the five-minute net-load forecast data of CAISO for Feb. 2, 2015 [26], scaled it down to the original IEEE-RTS peak load of 2850 MW, and generated the hourly day-ahead load forecast where the forecast standard deviation is considered to be %1 of the load at the time. Correspondingly, the ramping capability of IEEE-RTS units are scaled down with the ratio of twelve. The N_m^{00} and N_m^{10} coefficients of the cubic Hermite model of load respectively equal to the value of hourly load forecast at hours m and $m+1$ while the three-point finite difference method [24] is utilized to calculate the N_m^{01} and N_m^{11} coefficients. The two DA load profiles and their deviation from the RT load are shown in Fig. 4(a) and (b) respectively. The impact of solar generation on reducing the CAISO's load during sunlight and the resulting ramping events is obvious in Fig. 4(a). The errors shown in Fig. 4(b) are due to both the imperfect net-load forecast and the approximation error of the DA net-load profile. The latter is dominant in Case 1 with piecewise constant DA net-load approximation, where a significant amount of load is left out for RT operation.[1] The proposed cubic Hermite load model reduces the approximation error, embedding the sub-hourly variations in DA load profile.

The DA and RT simulation results for both cases are summarized in Table I. In Table I, the DA operation cost in the proposed UC model is increased by \$5,095.7, while the RT operation cost is reduced by \$10,651.6 (%63) as compared to Case 1, resulting in the total reduction of \$5,555.9 in daily operation cost in Case 2. In Fig. 4(b), the piecewise constant load profile used in traditional UC model leaves out a substantial amount of net-load for RT operation. The net-load presents several fast ramping events specially when the solar generation starts to rise in the early morning and suddenly drops during sunset. The substantial load deviation and several fast ramping events causes the relatively high RT operation cost for Case 1 in Table I. In addition, due to the lack of ramping capacity in RT operation, 27 ramping scarcity events are observed in Case 1; that is, the RT economic dispatch becomes infeasible due to insufficient ramping capacity of generation units, which reveals the inadequacy of the current UC model in accounting the sub-hourly variations of net-load. Thus, the RT operation cost is not defined for the 27 ramping scarcity events in Case 1. We used the average operation cost of other feasible intervals as the operation cost of 27 infeasible intervals. From the total RT operation of \$16,882.9 in Case 1, \$1,577.3 is related to the scarcity events. However, no violations of the power balance is observed in the RT operation of Case 2, which demonstrates the ability of the proposed UC model to effectively schedule the available ramping capability of units to cater to the fast ramping of the net-load. Note that consideration of additional scheduling stages between the day-ahead UC and RT economic dispatch may result in fewer real-time scarcity events in Case 1. However, this simulation assumption is equally applied for both cases and compares the results of the two methods under equal conditions, showcasing the ability of the proposed model to outperform the current practice.

TABLE I
SCHEDULING RESULTS

Case	DA Operation Cost (\$)	RT Operation Cost (\$)	Total DA and RT Operation Cost (\$)	RT Ramping Scarcity Events
Case 1	471,130.7	16,882.9	488,013.6	27
Case 2	476,226.4	6,231.3	482,457.7	0

The continuous-time generation trajectories for two cases are shown in Fig. 5, where the units are grouped to 9 groups with various capacities, costs and characteristics. In Fig. 5(a), the traditional way of interpreting the UC schedule provides a constant hourly setting for the generating units and results in a piecewise constant generation trajectory. In Fig. 5(b), the proposed UC model provides a continuous-time schedule for generating units which efficiently utilizes their ramping capability to follow the continuous-time variations of the net-load, while leaving less energy to schedule in the RT operation. In Case 1, a total of twenty units are committed, while in the proposed model in Case 2, additional five units are committed to secure adequate ramping capacity in the hours 1–3 when there is a fast ramp in the net-load. Moreover, in Case 2, the 197 MW units are not committed in the hours 16–24; instead the 100 MW units with more than twice the ramping capacity are kept on to also supply the fast ramping of net-load caused by solar generation during hours 6–16. This result highlights that consideration of sub-hourly ramping in day-ahead operation would modify the day-ahead commitment and schedule of generating units in such a way that the composition of online units is better prepared to respond to the sub-hourly variations of the net-load in real-time operation. So, it is of practical importance to account for the additional sub-hourly ramping of generating units in day-ahead operation.

[1]The choice of calculating the energy matching the hourly samples (or any other arbitrary point within the hour) could be improved and potentially replaced with an estimate of the hourly energy demand. However the curve is sufficiently smooth to make these difference negligible in the resulting schedule and cost. The advantage of this specific choice is that the first and the third Hermite coefficients in each interval are the same as the hourly load forecasts (at the ends of the interval) utilized in the traditional UC formulation, which is essential to make the two models comparable.

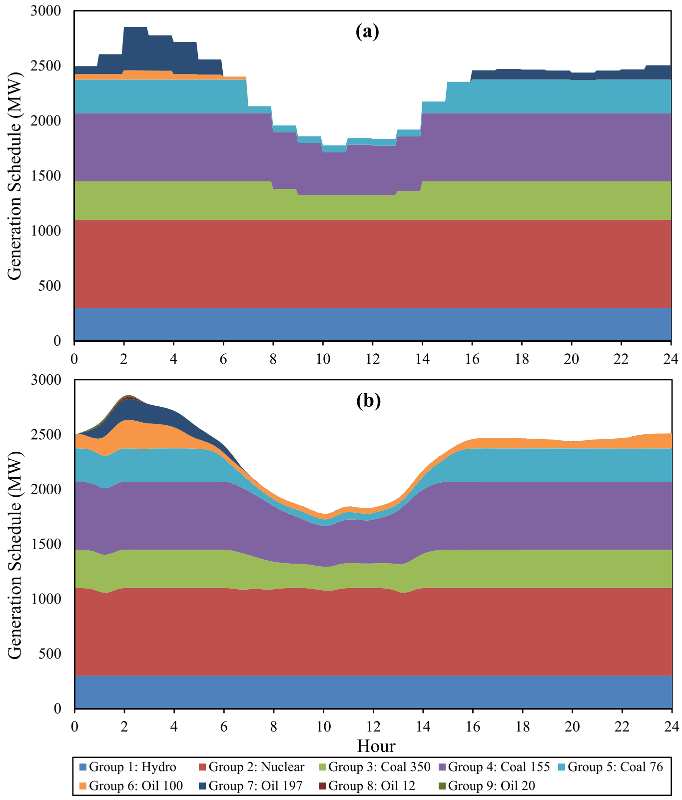

Fig. 5. DA Generation Trajectory in a) Case 1, b) Case 2.

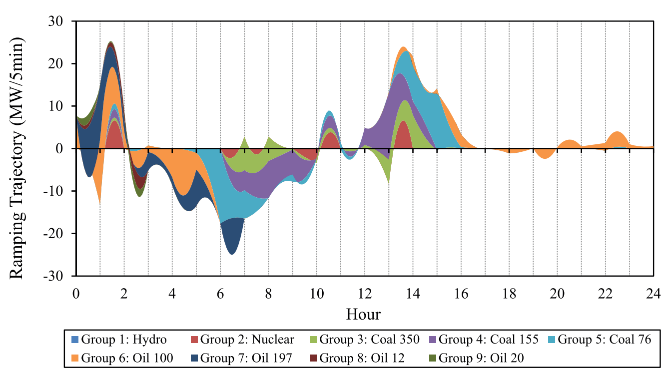

Fig. 6. Continuous-time ramping trajectory of units in Case 2.

The continuous-time ramping requirement of net-load and its breakdown to the scheduled ramping trajectory of generating units are shown in Fig. 6. In Fig. 6, the proposed UC model accounts for continuous-time ramping of load, which manifest several sub-hourly spikes, and schedules the generating units in day-ahead to deliver the continuous-time ramping requirement of load in real-time operation.

In order to evaluate the performance of our proposed model in different loading and forecast error conditions, we repeated the same Cases 1 and 2 in Fig. 7 for the CAISO's load data of the entire month of Feb. 2015 [26], and also added the results obtained from the traditional UC model with 48 half-hour periods. From the scatter diagram in Fig. 7(a), we can clearly see that our proposed UC model outperforms the other two cases in terms of real-time and total operation cost reduction, even compared to the half-hourly UC solution. Note that the latter

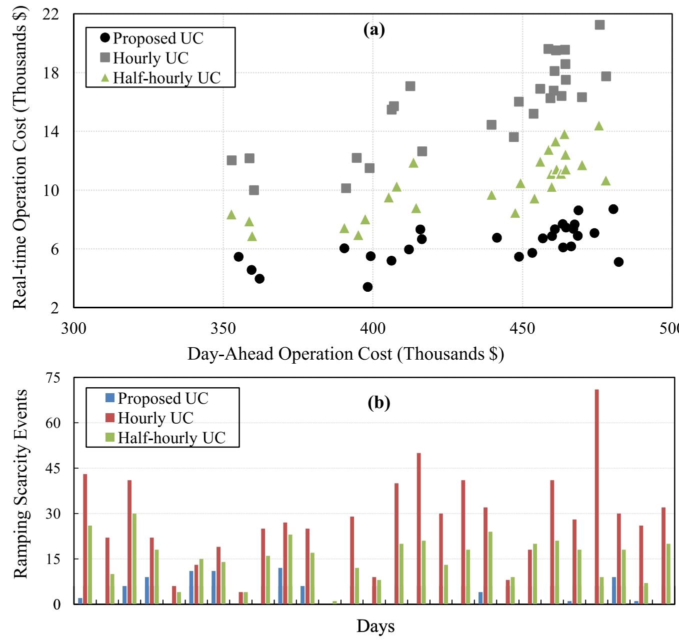

Fig. 7. Simulation of CAISO's load of Feb. 2015, a) DA vs RT operation costs, b) number of RT ramping scarcity events.

could have benefited from having twice the binary variables for half-hourly commitment status changes, which is prevented in this test for our model; this indicates that the brute-force solution of increasing the number of scheduling intervals is inferior compared to our solution. In addition, Fig. 7(b) reveals that our proposed UC model results in much fewer ramping scarcity events.

A. Computation Time

The computation time of simulating the day-ahead operation of IEEE-RTS with 32 generating units for the CAISO load data of Feb. 2, 2015, using the traditional 24-hour UC model, 48 half-hourly UC model, and the proposed function space-based UC model are respectively 0.257 s, 0.572 s, and 1.369 s, while the upper bound on the duality gap is set to be zero. The study cases were solved using CPLEX 12.2 [27] on a desktop computer with a 2.9 GHz i7 processor and 16 GB of RAM. Our proposed UC model has the same number of binary variables as compared to the traditional 24-hour UC model, but the reason for increased computation time is that it includes additional continuous variables, and equality and inequality constraints. The number of continuous generation variables is increased from 1 to 4 in each interval for each generating unit. The number of equality balance constraints is increased from 1 to 4 equality constraints in each interval. The number of inequality capacity and ramping constraints is increased from 2 and 2, respectively to 8 and 6 constraints in each interval for each generating unit. There are also additional two constraints in each interval for each generating unit enforcing the C^1 continuity of the generation trajectory. However, having the same number of binary variables is promising for large-scale implementation of our proposed model. In fact, the computation time of a MILP problem, due to the nature of branch-and-cut algorithm, is almost an exponential function with respect to the number of integer variables [28].

As highlighted in Remark IV.1, increasing the order of polynomials to approximate the load and model the continuous-time generation trajectory of units would increase the computation time of the problem. This is, however, an important feature of our proposed model that offers customizable levels of accuracy and computation complexity in approximating the decision space of day-ahead power system operation, which can be tuned by the system operator.

VII. Conclusion and Future Work

This paper introduces a new formulation of the day-ahead UC problem aimed at optimally scheduling of continuous-time generation and ramping trajectories of generating units. The proposed model preserves the MILP structure of current UC practice, with the same number of binary variables in the problem. Our numerical results on CAISO's real load data show that the commitment and schedule of the units in the proposed model is different from those of the current practice and that the application of proposed UC model has the potential of reducing significantly the number of ramping scarcity events in the real-time operation and of reducing the total operation costs.

In future work, one of the important features of our proposed ramping trajectory model that we will investigate is the definition of a ramping market because of the possibility of bidding on the ramping trajectory. In addition, consideration of transmission network power flow and constraints, inclusion of various reserve services, and definition of the associated market prices are in order. Also not considered in this work is how to appropriately tune the net-load forecasts and deal with uncertainty in the proposed UC model, which are natural extensions of the current framework and essential ones to fully cope with the stochastic nature of load and renewable energy resources.

Acknowledgment

The authors would like to thank the anonymous reviewers for their constructive comments and suggestions, which improved the clarity of the paper.

References

[1] M. Shahidehpour, H. Yamin, and Z. Li, *Market Operations in Electric Power Systems: Forecasting, Scheduling, and Risk Management*. New York, NY, USA: Wiley, 2002.

[2] J. M. Arroyo and A. J. Conejo, "Multiperiod auction for a pool-based electricity market," *IEEE Trans. Power Syst.*, vol. 17, no. 4, pp. 1225–1231, Nov. 2002.

[3] A. L. Motto, F. D. Galiana, A. J. Conejo, and J. M. Arroyo, "Network-constrained multiperiod auction for a pool-based electricity market," *IEEE Trans. Power Syst.*, vol. 17, no. 3, pp. 646–653, Aug. 2002.

[4] M. Carrión and J. M. Arroyo, "A computationally efficient mixed-integer linear formulation for the thermal unit commitment problem," *IEEE Trans. Power Syst.*, vol. 21, no. 3, pp. 1371–1378, Aug. 2006.

[5] B. Lu and M. Shahidehpour, "Unit commitment with flexible generating units," *IEEE Trans. Power Syst.*, vol. 20, no. 2, pp. 1022–1034, May 2005.

[6] M. Parvania and M. Fotuhi-Firuzabad, "Demand response scheduling by stochastic SCUC," *IEEE Trans. Smart Grid*, vol. 1, no. 1, pp. 89–98, 2010.

[7] M. R. Milligan, E. Ela, D. Lew, D. Corbus, and Y.-h. Wan, Advancing Wind Integration Study Methodologies: Implications of Higher Levels of Wind, National Renewable Energy Lab., 2010.

[8] M. Milligan *et al.*, "Operating reserves and wind power integration: An international comparison," in *Proc. 9th Int. Workshop Large-Scale Integration of Wind Power Into Power Systems*, 2010, pp. 18–29.

[9] U. Helman *et al.*, Integration of Renewable Resources: Operational Requirements and Generation Fleet Capability at 20% RPS, 2010.

[10] Growing Wind: Final Report of the Nyiso 2010 Wind Generation Study, 2010.

[11] J. Wang, M. Shahidehpour, and Z. Li, "Security-constrained unit commitment with volatile wind power generation," *IEEE Trans. Power Syst.*, vol. 23, no. 3, pp. 1319–1327, Aug. 2008.

[12] F. Bouffard and F. Galiana, "Stochastic security for operations planning with significant wind power generation," *IEEE Trans. Power Syst.*, vol. 23, no. 2, pp. 306–316, May 2008.

[13] N. Navid and G. Rosenwald, "Market solutions for managing ramp flexibility with high penetration of renewable resource," *IEEE Trans. Sustain. Energy*, vol. 3, no. 4, pp. 784–790, 2012.

[14] N. Navid and G. Rosenwald, "Ramp capability product design for MISO markets," *White Paper*, Jul. 2013.

[15] L. Xu and D. Tretheway, Flexible Ramping Products: Revised Draft Final Proposal, 2012.

[16] K. H. Abdul-Rahman, H. Alarian, M. Rothleder, P. Ristanovic, B. Vesovic, and B. Lu, "Enhanced system reliability using flexible ramp constraint in CAISO market," in *Proc. 2012 IEEE Power and Energy Soc. General Meeting*, 2012, pp. 1–6.

[17] C. Wang, P. Luh, and N. Navid, "Requirement design for a reliable and efficient ramp capability product," in *Proc. 2013 IEEE Power and Energy Soc. General Meeting*, 2013, pp. 1–5.

[18] N. A. Brown, V. Ajjarapu, and N. Navid, "Economic dispatch with deliverable ramping capability constraint for high wind penetration," in *Proc. 2014 IEEE Power and Energy Soc. General Meeting*, 2014, pp. 1–5.

[19] B. Wang and B. Hobbs, "Flexiramp market design for real-time operations: Can it approach the stochastic optimization ideal?," in *Proc. 2013 IEEE Power and Energy Soc. General Meeting*, 2013, pp. 1–5.

[20] A. A. Thatte, X. A. Sun, and L. Xie, "Robust optimization based economic dispatch for managing system ramp requirement," in *Proc. 47th Hawaii Int. Conf. System Sciences (HICSS)*, 2014, pp. 2344–2352.

[21] CAISO, Business Practice Manual for Market Operations, Sep. 30, 2014 [Online]. Available: http://caiso.com

[22] S. Mallat, *A wavelet Tour of Signal Processing*. New York, NY, USA: Academic, 1999.

[23] P. Dierckx, *Curve and Surface Fitting with Splines*. Oxford, U.K.: Oxford Univ. Press, 1993.

[24] P. Prenter, *Splines and Variational Methods*. New York, NY, USA: Dover, 2008.

[25] R. T. S. T. Force, "The IEEE reliability test system – 1996," *IEEE Trans. Power Syst.*, vol. 14, no. 3, pp. 1010–1020, Aug. 1999.

[26] California ISO Open Access Same-Time Information System (OASIS), Apr. 2015 [Online]. Available: http://oasis.caiso.com

[27] CPLEX 12.2 Manual. Armonk, NY, USA, IBM Corp., 2011.

[28] T. Li and M. Shahidehpour, "Price-based unit commitment: A case of Lagrangian relaxation versus mixed integer programming," *IEEE Trans. Power Syst.*, vol. 20, no. 4, pp. 2015–2025, Nov. 2005.

Masood Parvania (M'14) is an Assistant Professor and the director of the U-Smart lab at the Department of Electrical and Computer Engineering at the University of Utah. His research interests include the operation and planning of power and energy systems, modeling and integration of distributed energy resources, as well as sustainable renewable energy integration.

Dr. Parvania is currently the Chair of the IEEE Power and Energy Society (PES) Task Force on Reliability Impacts of Demand Response Integration, and the Secretary of the IEEE PES Reliability, Risk and Probability Application (RRPA) Subcommittee.

Anna Scaglione (F'11) is a Professor in Electrical, Computer and Energy Engineering at Arizona State University. Her expertise is in the broad area of signal processing for communication and power systems.

Dr. Scaglione was Editor-in-Chief of the IEEE Signal Processing Letters, and was in the Board of Governors of the Signal Processing Society from 2012 to 2014. She is recipient of the 2013 IEEE Donald G. Fink Prize Paper Award, the 2013 SPS Young Author best paper award (with her student), the 2000 IEEE Signal Processing Transactions Best Paper Award, the SmartGridcomm 2014 Best Student Paper Award, the Ellersick Best Paper Award (MILCOM 2005) and the NSF Career Award in 2002.